Chemosphere 138 (2015) 47–59

Contents lists available at ScienceDirect

Chemosphere

journal homepage: www.elsevier.com/locate/chemosphere

Microbial community composition of a household sand filter used for arsenic, iron, and manganese removal from groundwater in Vietnam

Katja Sonja Nitzsche [a], Pascal Weigold [a], Tina Lösekann-Behrens [b], Andreas Kappler [a], Sebastian Behrens [b,*]

[a] Geomicrobiology/Microbial Ecology, Center for Applied Geoscience, Eberhard Karls University Tübingen, Germany
[b] Department of Civil, Environmental, and Geo-Engineering, University of Minnesota, USA

HIGHLIGHTS

- We studied the microbial community composition of a household sand filter for arsenic removal from groundwater.
- Mn-oxidizing bacteria were enriched in a distinct filter layer.
- The microbial community on the filter was dominated by nitrifying microorganisms.
- Abiotic iron oxidation prevailed over biotic Fe(II) oxidation.
- The formation of Mn oxides contributed to abiotic As oxidation and immobilization by sorption to Fe oxides.

ARTICLE INFO

Article history:
Received 25 December 2014
Received in revised form 24 April 2015
Accepted 8 May 2015

Keywords:
Iron oxidation
Manganese oxidation
Arsenite oxidation
Ammonia oxidation
Water filtration
Drinking water

ABSTRACT

Household sand filters are used in rural areas of Vietnam to remove As, Fe, and Mn from groundwater for drinking water purposes. Currently, it is unknown what role microbial processes play in mineral oxide formation and As removal during water filtration. We performed most probable number counts to quantify the abundance of physiological groups of microorganisms capable of catalyzing Fe- and Mn-redox transformation processes in a household sand filter. We found up to 10^4 cells g^{-1} dry sand of nitrate-reducing Fe(II)-oxidizing bacteria and Fe(III)-reducing bacteria, and no microaerophilic Fe(II)-oxidizing bacteria, but up to 10^6 cells g^{-1} dry sand Mn-oxidizing bacteria. 16S rRNA gene amplicon sequencing confirmed MPN counts insofar as only low abundances of known taxa capable of performing Fe- and Mn-redox transformations were detected. Instead the microbial community on the sand filter was dominated by nitrifying microorganisms, e.g. *Nitrospira*, *Nitrosomonadales*, and an archaeal OTU affiliated to *Candidatus* Nitrososphaera. Quantitative PCR for *Nitrospira* and ammonia monooxygenase genes agreed with DNA sequencing results underlining the numerical importance of nitrifiers in the sand filter. Based on our analysis of the microbial community composition and previous studies on the solid phase chemistry of sand filters we conclude that abiotic Fe(II) oxidation processes prevail over biotic Fe(II) oxidation on the filter. Yet, Mn-oxidizing bacteria play an important role for Mn(II) oxidation and Mn(III/IV) oxide precipitation in a distinct layer of the sand filter. The formation of Mn(III/IV) oxides contributes to abiotic As(III) oxidation and immobilization of As(V) by sorption to Fe(III) (oxyhydr)oxides.

1. Introduction

In many regions of South and South-East Asia, groundwater aquifers contain high concentrations of arsenic (As) (Mandal and Suzuki, 2002; Muehe and Kappler, 2014). Due to the chronic health effects associated with prolonged exposure to As-rich drinking water, the world health organization set the drinking water limit to 10 μg L^{-1} in 1993. Groundwater aquifers in South and South-East Asia often also contain high concentrations of dissolved iron (Fe) and manganese (Mn), which affect the taste and visual nature of the drinking water (Buschmann et al., 2007; Hug et al., 2008; Winkel et al., 2011). In rural areas of Vietnam, household sand filters have been established as cost-efficient and effective solution for the removal of As, Fe, and Mn from groundwater (Fig. 1). Previous studies have shown that at groundwater Fe/As ratios above 250 (weight based), sand filters can effectively reduce As concentrations in the filtered water to levels below 10 μg L^{-1} (Berg et al., 2006; Nitzsche et al., 2015).

* Corresponding author at: Department of Civil, Environmental, and Geo-Engineering, University of Minnesota, 500 Pillsbury Drive S.E., Minneapolis, MN 55455-0116, USA.
E-mail address: sbehrens@umn.edu (S. Behrens).

http://dx.doi.org/10.1016/j.chemosphere.2015.05.032
0045-6535/

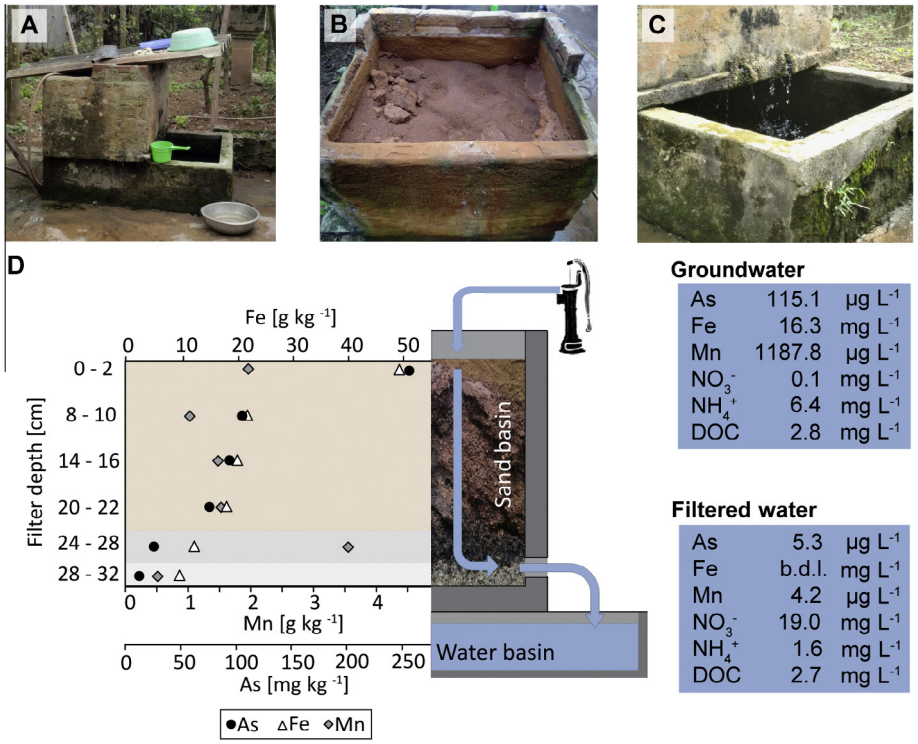

Fig. 1. Household sand filters used for arsenic, iron, and manganese removal from groundwater in Vietnam. (A) Shows a typical sand filter widely used in the Red River Delta in Vietnam. The sand filter consists of two basins stacked on top of each other. The upper basin is filled with sand and the lower basin serves as water storage container. The groundwater is pumped from a shallow tube well onto the filter, trickles though the sand column, and is collected in the bottom tank. (B) Top view on the sand filled upper basin and (C) water trickling into the storage container via holes in the bottom of the upper sand filled basin. (D) Schematic cross section of the sand filter showing a depth profile of the filter sand which is colored due to the precipitation and coating of sand particles with red-brown Fe(III) (oxyhydr)oxides (depth of 0–23 cm) and black Mn(IV) oxides (depth of 23–28 cm). The bottom sand layer (depth of 28–32 cm) shows the initial color of the filter sand. Diagram shows a depth profile of accumulated As, Fe, and Mn in the different colored sand layers quantified by XRF (Nitzsche et al., 2015). Blue boxes show concentrations of As, Fe, Mn, NO_3^-, NH_4^+ and DOC in the groundwater before and after filtration (b.d.l. = below detection limit) (Nitzsche et al., 2015).

The geochemical processes for the removal of As, Fe, and Mn from anoxic groundwater in aerated sand filters are well known: Dissolved Fe(II) is oxidized which leads to the formation of poorly soluble Fe(III) (oxyhydr)oxide minerals on the sand particles (Jessen et al., 2005; Voegelin et al., 2014). Fe(II) oxidation at neutral pH can result from homogeneous oxidation of dissolved Fe(II) by oxygen, heterogeneous oxidation of Fe(II) driven by catalytic surfaces reactions, and under microaerophilic oxygen concentrations by microbial Fe(II) oxidation (van Beek et al., 2012; Melton et al., 2014b). The abiotic Fe oxidation also causes co-oxidation of As(III) to As(V) which equally well or even more strongly adsorb to the newly formed Fe(III) (oxyhydr)oxide precipitates at pH >8 than As(III) (Dixit and Hering, 2003). Homogeneous Mn oxidation by oxygen at neutral pH is relatively slow, so that the formation of soluble Mn(III/IV) oxides occurs mainly as result of heterogeneous and microbial Mn oxidation (Tebo et al., 2004; Learman et al., 2011; Luan et al., 2012). Both Mn(III) and Mn(IV) oxides can function as oxidants for Fe(II) (Postma, 1985; Villinski et al., 2001) and As(III) (Tournassat et al., 2002; Ying et al., 2012). The formation of Mn oxides on the sand filter will therefore improve As and Fe removal from the filtered water (Nitzsche et al., 2015). A black Mn oxide layer developed when most of the reduced Fe and As has been removed from the groundwater (Nitzsche et al., 2015). The Mn oxide layer is therefore indicative for a transition zone below which Fe and As concentrations in the filtered water are considerably reduced.

Although much is known about the abiotic processes contributing to the performance of sand filters and their As, Fe, and Mn removal efficiency (Voegelin et al., 2014; Nitzsche et al., 2015), the composition of the microbial community and the potential contribution of different physiological groups of microorganisms to the removal of As, Fe, and Mn have not been investigated for household sand filters in Vietnam to date. Anoxic groundwater becomes aerated during filtration and oxic/anoxic interfaces at the surface of sand particles might allow Fe(II)-oxidizing bacteria to successfully compete with slower abiotic Fe(II) oxidation rates at reduced oxygen concentrations (Emerson and Moyer, 1997). Microbial As(III) respiration and/or detoxification mechanisms could affect As redox speciation on the filter and simultaneously sustain and secure the survival of a metabolically diverse microbial community (Oremland and Stolz, 2003). In addition, the slow kinetics of purely abiotic surface-catalyzed Mn(II) oxidation suggests that Mn(II)-oxidizing bacteria might be contributing to Mn removal in sand filters (Tebo et al., 2004; Voegelin et al., 2014). Previous studies have mostly relied on conventional molecular techniques (e.g. DGGE, T-RFLP) to describe the diversity and distribution of microorganisms in lab or full-scale biofilters for the simultaneous removal of As, Fe, Mn or ammonium (NH_4^+) from groundwater (Li et al., 2013; Yang et al., 2014), but no studies on sand filters used in actual households are available.

The aim of the present study therefore was a comprehensive and quantitative analysis of the composition and depth distribution of the microbial community in a sand filter, used by a rural household in Vietnam. More specifically, we performed most probable number (MPN) counts to quantify the number of microaerophilic and nitrate-reducing Fe(II)-oxidizing bacteria, Fe(III)-reducing bacteria, as well as Mn(II)-oxidizing, and Mn(IV)-reducing bacteria in both water samples and different

depth layers of the sand filter. MPN counts were correlated to X-ray fluorescence (XRF) data on the distribution of Fe and Mn in the sand filter. 454 pyrosequencing of 16S rRNA gene amplicons of bacteria and archaea was used to analyze the microbial community composition in different depth layers of the sand filter, the groundwater, the filtered water, and the original sand used to construct the filter. Quantitative PCR (qPCR) using general and group-specific primers for selected 16S rRNA gene taxa and functional genes was also applied and used to independently verify results of the MPN and amplicon sequencing analyses.

2. Material and methods

2.1. Sand filter description

The study was performed on a representative sand filter in the village Van Phuc, Province Hanoi, in Vietnam (Fig. 1). The investigated sand filter is representative for sand filters used in Northern Vietnam in terms of shape, size, material, filter velocity, filter usage and capacity for As and Fe removal (M. Berg *personal communication*, Berg et al., 2006; Nitzsche et al., 2015). The sand filter is located in an area with As groundwater concentrations <100 $\mu g\,L^{-1}$ (Berg et al., 2008). The sand filter was built at the end of the 1990s and since then, has been used by one family several times per day (Nitzsche et al., 2015). The sand basin dimensions were 83 cm × 57 cm × 52 cm and the basin contained approximately 0.20 m^3 of fine gravel to very fine sand (Voegelin et al., 2014). The sand was collected from the local river banks of the Red River and was in use for more than 8 years prior to sampling. The sand filter significantly reduces As, Fe, and Mn concentrations in the filtered groundwater as described in detail previously (Nitzsche et al., 2015) (Fig. 1D). Groundwater filtration leads to the accumulation of As, Fe, and Mn at different depth layers in the sand, which are also characterized by distinct color changes ranging from; red-brown poorly crystalline Fe(III) oxyhydroxides (0–23 cm depth, from here on referred to as "red layer"), to black Mn oxide minerals (24–28 cm, from here on referred to as "black layer"), to a white sand layer at the bottom of the filter (28–32 cm, from here on referred to as "white layer", which had the appearance of the original sand used to construct the filter (Nitzsche et al., 2015)) (Fig. 1D). A depth distribution of total As, Fe, and Mn in the sand filter determined by XRF can be found in Fig. 1D. The highest concentrations of As (260 $mg\,kg^{-1}$) and Fe (49 $g\,kg^{-1}$) were quantified in the top 2 cm of the red layer and decreased with filter depth down to the white layer (As 6 $mg\,kg^{-1}$ and Fe 8 $g\,kg^{-1}$). Arsenic and Fe concentrations showed a linear correlation throughout filter depth. Mn concentrations were highest (1135 $mg\,kg^{-1}$) in the black layer (Nitzsche et al., 2015). Further details on the bulk and micro-scale characterization of the solid phase of the filter, the effect of filter usage practices on As removal efficiency, the microbiological water quality, and the geochemical composition of the groundwater and filtered water have been described in detail in Voegelin et al. (2014) and Nitzsche et al. (2015).

2.2. Sand filter sampling

Sampling of the sand filter for microbial community analysis was performed in 2012. The sand filter was chosen to complement previous studies on the geochemistry and performance conducted of the same sand filter by Voegelin et al. (2014) and Nitzsche et al. (2015) who focused solely on As, Fe, and Mn removal efficiency form the groundwater.

Groundwater samples (from here on referred to as sand filter "inflow water") and samples from the freshly filtered water (from here on referred to as sand filter "outflow water") were collected in sterile 50 mL tubes and immediately cooled on ice during transport to the lab for MPN analysis. Water samples (100 mL each) for DNA extractions were filtered through polyethersulfone (PES) membrane filters (0.22 μm Express® Plus Membrane, Millipore). The samples were collected at three consequent days in duplicate and the filters were cooled on ice during transport to the laboratory.

Sand from the filter was collected for geochemical analyses, MPN counts, and DNA extraction by manually digging a hole using a plastic scoop in the middle of the sand filter. Bulk sand samples were then taken from six different depths (0–2 cm, 8–10 cm, 14–16 cm, 20–22 cm, 24–28 cm, and 28–32 cm) by pushing three 50 mL plastic tubes (standard sized screw cap, sterile Falcon tubes) per layer horizontally into the exposed sand profile. Three samples from the original sand were also collected in 50 mL plastic tubes. All sand samples were immediately cooled on ice for transport. Upon arrival at the laboratory of Hanoi University (Vietnam) water and sand samples were either frozen at −20 °C (for DNA extraction), or stored at 4 °C (for MPN inoculation and geochemical analyses).

2.3. Geochemical characterization of the filter sand

Water content, pH, and total organic carbon (TOC) were determined from the filter sand as described in the supporting information (SI).

2.4. Most-probable-number (MPN) counts

MPN counts were performed on inflow and outflow water samples, sand collected from the different filter depths, and the original sand. MPNs on liquid medium were set up in 96-well plates for the quantification of nitrate-reducing Fe(II)-oxidizing bacteria (NredIOB), Fe(III)-reducing bacteria (IRB), Mn(II)-oxidizing bacteria (MOB), and Mn(IV)-reducing bacteria (MRB) as described in Melton et al. (2014a), Straub et al. (2005), and Tebo et al. (2007). Microaerophilic Fe(II)-oxidizing bacteria (mIOB) were quantified in agar gradient tubes (Emerson and Merrill Floyd, 2005). Detailed descriptions of the medium recipes for the different physiological groups, substrate concentrations, incubation conditions, and proof of bacterial growth are provided in the SI. Cell numbers (cells g^{-1} dry sand) from the positive MPN wells/tubes were calculated using the software program KLEE applying confidence limits of Cornish and Fisher (1938) and the bias correction after Salama (1978) as previously described (Klee, 1993).

2.5. DNA extraction

Prior to DNA extraction frozen sand cores were cut into sections using a band saw and only sand from the inner part of each core layer was used for molecular analysis after thawing and homogenization. For sequencing and qPCR analyses, DNA from water samples (concentrated biomass on membrane filters) and filter sand were extracted using the PowerWater® and PowerSoil® DNA Isolation Kits (MoBio Laboratories), respectively. Extraction protocols followed the manufacturer's instructions. For sequencing of 16S rRNA gene amplicons from the filter sand, DNA was also extracted following the soil DNA extraction protocol published by Zhou et al. (1996) with further purification of the obtained genomic DNA using the QIAEX II Agarose Gel Extraction kit (QIAGEN). DNA extractions of the sand were performed in

duplicates for each sample and extraction method and later the extracted DNA was pooled. DNA extracts of duplicate water samples taken at three consecutive days were pooled before further analyses. DNA concentration and quality were determined spectrophotometrically (NanoDrop 1000, Thermo Scientific) and by agarose gel electrophoresis.

2.6. Sequencing of 16S rRNA gene amplicons

Bacterial 16S rRNA genes were amplified using the primers 27F (5′-AGAGTTTGATCMTGGCTCAG-3′) (Lane, 1991) and 534R (5′-ATTACCGCGGCTGCTGGC-3′) (Muyzer et al., 1993; Liu et al., 2007) targeting the V1–V3 region of the 16S rRNA gene. The V6–V8 region of the archaeal 16S rRNA gene was amplified using the primers 958F (5′-AATTGGANTCAACGCCGG-3′) (DeLong, 1992) and 1392R (5′-ACGGGCGGTGTGTRC-3′) (Pace et al., 1986). Primers 27F and 958F contained Roche 454 pyrosequencing barcodes and adaptor A, primers 534R and 1392R contained adaptor B. PCR reactions were performed in duplicates for each sample and each of the two DNA extracts using the FastStart High Fidelty PCR reagents (Roche) PCR conditions are described in the supporting information. PCR products were pooled in equimolar concentrations. The quality of the amplified DNA was confirmed on an Experion® automated electrophoresis system (Bio-Rad). Prior to sequencing, the PCR products were quantified using the Quant-iT™ PicoGreen® dsDNA assay kit (Invitrogen) and a QuantiFluor®-ST fluorometer (Promega). 454 pyrosequencing was performed on a Roche GS Junior Sequencer (454 Life Sciences) according to the manufacturer's instructions for amplicon sequencing. We sequenced a synthetic 'mock' community of known species composition containing Archaea and Bacteria to evaluate the efficiency and accuracy of library preparation, pyrosequencing, and amplicon classification. Following sequence analysis we were able to correctly assign sequence reads and reproduce the composition of the 'mock' control community.

2.7. Sequence analysis

Quality control, alignment and classification of the sequencing data were performed using the software package MOTHUR, version v.1.32.0 (Schloss et al., 2009). Pyrosequencing noise and chimeras were removed with the in MOTHUR implemented algorithms PyroNoise (Quince et al., 2009) and UCHIME (Edgar et al., 2011) as described previously (Schloss et al., 2011). Sequences shorter than 200 bp and sequences with homopolymers longer than 8 bp were removed from the dataset. The remaining sequences were aligned against the SILVA SSU Ref rRNA database (v.102) (Pruesse et al., 2007) and pre-clustered with the single-linkage algorithm applying a threshold of 2% (Huse et al., 2010). A distance matrix was created and sequences were assigned to operational taxonomic units (OTUs) based on 97% sequence identity using the average neighbor algorithm (Schloss and Westcott, 2011). Sequences were classified using the Naïve Bayesian Classifier (Wang et al., 2007) and the SILVA reference taxonomy applying a minimum bootstrap confidence cutoff of 60%. Random subsampling was performed to normalize the dataset to the sample with the lowest number of reads (for bacteria $n = 2703$ and for archaea $n = 2527$). Cluster analysis on samples was performed using an Unweighted Pair Group Method with Arithmetic Mean (UPGMA) algorithm and was based on calculated Bray–Curtis dissimilarities between the samples (Bray and Curtis, 1957). Rarefaction curves, the richness estimator Chao1, the abundance-based coverage estimator (ACE), and the diversity indices Shannon (H́) and Simpson (D) were calculated based on 97% sequence similarity using MOTHURs implementation DOTUR (Schloss and Handelsman, 2005). Heatmaps were created by importing relative abundance data of relevant taxa of the different samples into RStudio, version v0.98.501 and normalized by calculating *Z*-scores. The *Z*-score represents the number of standard deviations the relative abundance of taxa in a specific sample differ from the mean relative abundance of that taxa in all samples.

Pyrosequencing reads were deposited at the European Nucleotide Archive under accession number PRJEB8996.

2.8. Quantitative polymerase chain reaction (qPCR)

Quantitative PCRs were performed using general 16S rRNA gene primers for Bacteria and Archaea, and specific 16S rRNA gene primers for the taxa *Nitrospira*, *Gallionellales*, and *Geobacteraceae*. In addition functional gene qPCRs targeting bacterial and archaeal ammonia monooxygenases (*amoA*) were performed. qPCR primer sequences, gene-specific plasmid standards, and details of the thermal programs are given in the SI (Table SI 1). qPCR reactions were carried out in 20 μL volume containing 10 μL 1x SsoFast™ Eva Green® Supermix (Bio-Rad), gene specific primers (concentrations given in Table SI 1), PCR water, and 2 μL of either standard plasmid DNA (ten-fold dilution series) or sample DNA (10–100 ng μL^{-1}). Thermal programs were run on an iQ5 real-time PCR detection system (Bio-Rad). Each DNA extract was quantified in triplicates and gene copy numbers were calculated from two independent DNA extracts. Raw data were background subtracted using the iQ™5 optical system software 2.0 (Bio-Rad Laboratories) and exported from the iCyler system and analyzed using the software Real-Time PCR Miner (Zhao and Fernald, 2005). Further data analysis and gene copy number calculations were done as described by Behrens et al. (2008).

3. Results

3.1. Characterization of the sand filter, groundwater and filtered water

The filter sand as well as the groundwater, and the filtered water have been well characterized in two recent studies (Voegelin et al., 2014; Nitzsche et al., 2015). Additionally, we determined pH, water content, and TOC of the filter sand in this study (Table SI 2). The pH did not change significantly with filter depth and ranged between 7.5 and 7.6. The water content was highest in the black Mn(III/IV) oxide layer (19.5 ± 3.2%) and ranged between 5.0 ± 1.2% and 11.6 ± 1.5% in the other sand layers. The water content of the original sand was 0.3 ± 0.2%. The total organic carbon content was always below 0.1 weight% throughout the whole filter.

3.2. Microbial biomass distribution

In order to approximate total cell numbers and microbial biomass distribution in the sand filter we quantified bacterial and archaeal 16S rRNA gene copy numbers by qPCR (Fig. 2A). Bacterial 16S rRNA gene copy numbers ranged from $5 \pm 3 \times 10^6$ to $3 \pm 2 \times 10^8$ 16S rRNA gene copies g^{-1} dry sand. Archaeal 16S rRNA gene copy numbers ranged from $7 \pm 4 \times 10^5$ and $43 \pm 3 \times 10^6$ 16S rRNA gene copies g^{-1} dry sand. The depth distribution of both, bacterial and archaeal 16S rRNA gene copy numbers, followed the same trend. The sum of bacterial and archaeal 16S rRNA gene copy numbers only slightly changed in the first 16 cm of the sand filter (2 to 3×10^8 16S rRNA gene copies g^{-1} dry sand). Total 16S rRNA gene copy numbers then dropped to 6×10^6 16S rRNA gene copies g^{-1} dry sand in the layer from 20 to 22 cm and increased again to 3×10^8 16S rRNA gene copies g^{-1} dry sand toward the bottom of the sand filter (28–32 cm) (Fig. 2A). Archaeal 16S rRNA gene copies contributed with 3–16% to the total 16S rRNA gene copies quantified in the different sand

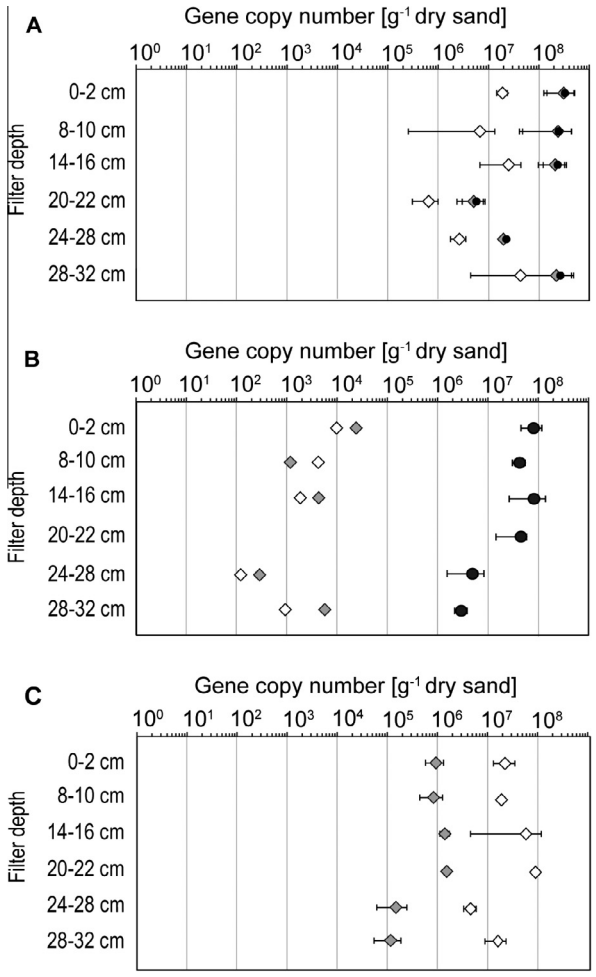

Fig. 2. Gene copy numbers per gram dry sand of the filter. (A) 16S rRNA gene copy numbers of Bacteria (gray diamonds), Archaea (white diamond), and total 16S RNA gene copy numbers (black circles, sum of 16S rRNA gene copy numbers of Bacteria and Archaea). (B) 16S rRNA copy numbers of *Geobacteraceae* (gray diamond), *Gallionellales* (white diamond), and *Nitrospira* sp. (black circle). (C) Functional gene copy numbers of bacterial (gray diamond) and archaeal (white diamond) ammonia monooxygenases. Given are mean values and the upper and lower range of two independent DNA extractions each quantified in triplicate qPCR reactions.

filter layers. The ratio of archaeal to bacterial 16S rRNA gene copies increased with filter depth (0.03–0.2) and was highest below the black Mn(III/IV) oxide layer. The original sand contained 7×10^7 total 16S rRNA gene copies g^{-1} dry sand of which only 1% accounted for archaeal 16S rRNA gene copies.

3.3. MPNs

MPN counts for NredIOB and IRB ranged from 10^2 to 10^3 and 10^2 to 10^4 cells g^{-1} dry sand, respectively (Fig. 3A). We did not observe any growth of microaerophilic IOB in gradient tubes in any of the sand filter samples. MPN counts for MOB were highest in the black layer from 24 to 28 cm (>3×10^6 cells g^{-1} dry sand) (Fig. 3B). In all other sand filter layers MOB MPN counts did not exceed 10^3 cells g^{-1} dry sand. MPN counts for MRB slightly decreased from 10^3 cells g^{-1} dry sand in the upper filter part (0–16 cm) to 10^2 cells g^{-1} dry sand below 20 cm. In the MPNs inoculated with inflow water and outflow water no growth of IOB, IRB, and MOB could be detected but MRB accounted for 10^2 cells L^{-1} in the inflow water (data not shown). In the original sand all five different physiological groups were quantified to be present with 10^1 cells g^{-1} dry sand (data not shown).

3.4. Microbial community composition

A total of 138,590 16S rRNA gene pyrosequencing reads were obtained from 9 different samples after quality processing of the raw sequence data with MOTHUR (samples from 6 different sand filter layers, the inflow and outflow water, and the original sand). In total 69,221 bacterial and 69,369 archaeal sequences with read lengths ranging from 230 to 280 bp were used for operational taxonomic unit assignment using a sequence similarity of 97% (Tables SI 3 and 4). Analysis of the synthetic 'mock' community revealed that bacterial and archaeal sequence reads could be correctly classified and that we were able to reproduce the composition of the 'mock' control community by our sequence analysis pipeline.

Rarefaction analyses are summarized in Fig. SI 1. Sequencing retrieved 50–60% of the bacterial richness and 33.6–85.7% of the archaeal richness estimated by Chao1. Based on different alpha-diversity indexes (Shannon and Simpson), the microbial diversities in the upper sand filter layers (down to 22 cm) were lower than within (24–28 cm) and below the black Mn(III/IV) oxide layer (28–32 cm) (Tables SI 3 and SI 4). The red layers from 0 to 22 cm contained on average 526 ± 58 different bacterial OTUs, while in and below the black Mn(III/IV) oxide layer the number of OTUs assigned was almost twice as high (989 ± 107 OTUs). Archaeal OTU numbers followed the same trend. They were with 25 ± 3 OTUs almost three times lower in the red layer than in the black and white sand layers, where 74 ± 6 OTUs were detected. Alpha diversity indexes also revealed a higher bacterial and archaeal diversity in the inflow and outflow water samples, and the original sand compared to the microbial community diversity of the different sand filter layers (Tables SI 3 and SI 4).

Microbial community compositions among the sand filter samples, the water inflow and outflow water samples, and the original sand were compared using UPGMA cluster analysis based on calculated Bray–Curtis dissimilarities between the samples (Fig. 4). A clear shift in the bacterial and archaeal community structures was observed among the sand filter samples taken at different filter depth with the most pronounced differences in microbial community structure between the sand filter layers above and below the Mn(III/IV) oxide layer at 24–28 cm. While the inflow and outflow water samples clustered together and were distinctly set off the sand samples, the microbial community structure of the original sand sample most closely resembled the bottom white sand layer of the filter.

3.5. Bacterial diversity

OTUs assigned to the phyla *Proteobacteria* (33 ± 3% relative sequence abundance) and *Nitrospirae* (36 ± 6%) were the most abundant bacterial taxa in the sand filter (Fig. 4A). Together their relative abundance accounted for 70–75% of all bacterial 16S rRNA gene sequences in the red layers (0–22 cm), and 55% and 60% in the black (24–28 cm) and white (28–32 cm) sand layers, respectively. The dominant class among the *Proteobacteria* in the sand filter were the *Betaproteobacteria* comprising the families *Nitrosomonadaceae*, *Comamonadaceae*, and *Rhodocyclaceae* (Fig. 5A). OTUs assigned to the ammonia-oxidizing *Nitrosomonas* were the dominant *Nitrosomonadaceae* population in the red sand layers (0–22 cm) (Fig. 5A). Taxa belonging to the betaproteobacterial families *Comamonadaceae* (such as *Delftia*) and *Rhodocyclaceae* were most abundant in a distinct sand filter layer from 20 to 22 cm. In total 16 OTUs were assigned to the phylum *Nitrospirae* of which one OTU accounted for 95 ± 3% of all *Nitrospirae* sequences in the sand filter (Fig. SI 2). This particular OTU was most closely related to the nitrite-oxidizer "*Candidatus* Nitrospira defluvii" (99% sequence identity). The dominant *Nitrospira defluvii*-related OTU was most abundant in the red sand layers (Fig. 5A). Although we

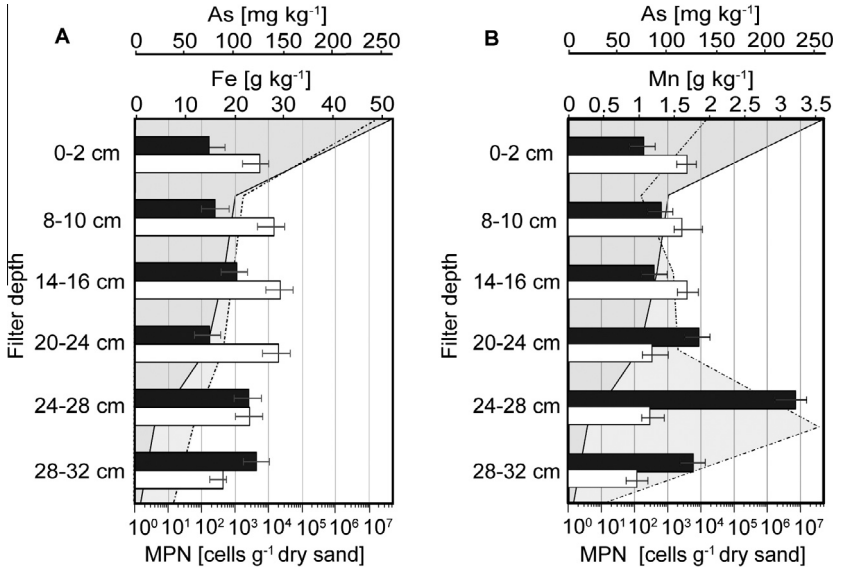

Fig. 3. Most probable number (MPN) counts from the sand filter. MPNs of (A) nitrate-reducing Fe(II)-oxidizing bacteria (NredIOB, black bars) and iron(III)-reducing bacteria (IRB, white bars) and (B) Mn(II)-oxidizing bacteria (MOB, black bars) and Mn(IV)-reducing bacteria (MRB, white bars). MPN counts are corrected after Salama (1978) and confidence limits given after Cornish and Fisher (1938). The gray shaded areas in the background show the concentrations of As (solid line) and in (A) Fe concentrations (dashed line) and in (B) Mn concentrations (dashed line) as determined by X-ray fluorescence by Nitzsche et al. (2015).

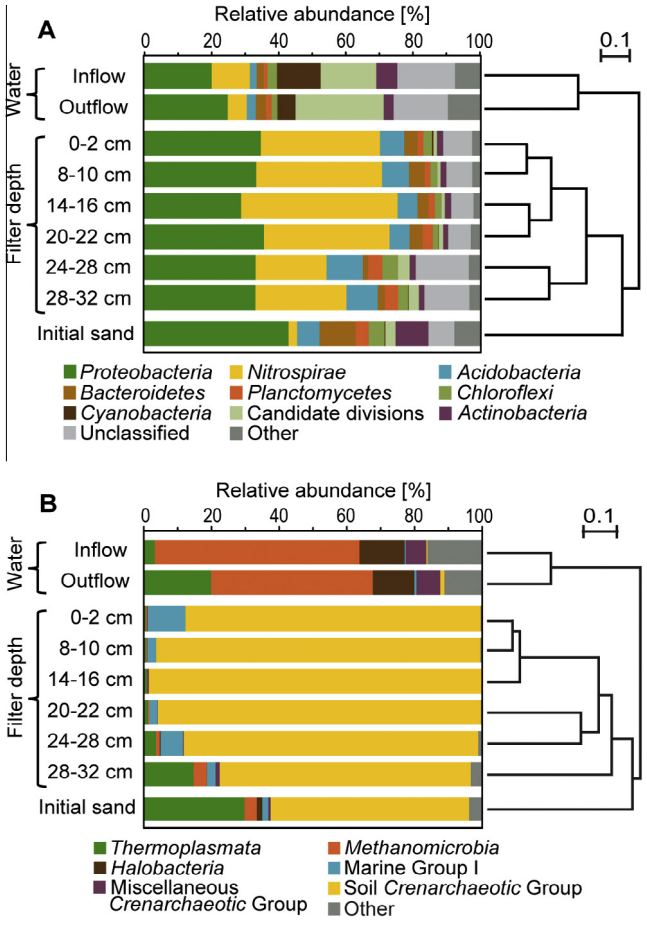

Fig. 4. Microbial community composition and similarity of water, filter sand, and original sand. Relative abundances and hierarchical clustering of (A) bacterial and (B) archaeal partial 16S rRNA gene sequences based on 97% sequence similarity. Cluster analyses were performed based on an UPGMA algorithm and Bray–Curtis dissimilarity. Relative sequence abundances are shown on the phylum level for (A) Bacteria and on the class level for (B) Archaea.

also detected *Nitrosomonas* and *Nitrospira* in the black and white sand filter layers, as well as in the water samples and the original sand, they were most dominant in the red sand filter layers.

The major populations in the inflow and outflow water samples were associated with OTUs belonging to the phyla *Proteobacteria* (20% inflow/25% outflow), *Cyanobacteria* (13%/5%), *Nitrospirae* (6%/11%), and the candidate divisions OP3 and OD1 (together 17%/26%) (Fig. 4A). While sequences of *Proteobacteria* and *Nitrospirae*-related OTUs were also found in significant abundance on the sand filter, sequences of OTUs belonging to the phyla *Cyanobacteria* and the candidate divisions OP3 and OD1 were most abundant in the water samples (Fig. 5A). OTUs belonging to the candidate divisions OD1 were also present in the original sand. The original sand was dominated by sequences of OTUs affiliated to the phyla *Proteobacteria* (43%), *Bacteroidetes* (11%), *Actinobacteria* (10%), and *Acidobacteria* (8%) (Fig. 4A). The prevalent proteobacterial OTUs in the original sand belonged to the orders *Rhizobiales* (*Alphaproteobacteria*), *Burkholderiales* (*Betaproteobacteria*), and *Xanthomonadales* (*Gammaproteobacteria*). The *Bacteroidetes* were represented by OTUs affiliated to the *Chitinophagaceae* (order *Sphingobacteriales*) (Fig. 5A).

Across all samples between 7% and 17% of the obtained bacterial sequence reads could not be classified on the phylum level.

3.6. Archaeal diversity

Most archaeal OTUs in the sand filter were assigned to the phylum *Crenarchaeota* while sequences of OTUs belonging to the phylum *Euryarchaeota* dominated in the water samples (Fig. 4B). The most abundant sequences in the filter sand were affiliated to the Soil *Crenarchaeotic* Group (SCG). Unclassified sequences within the SCG were highly abundant in the red sand filter layers (84 ± 4%). The black and white sand filter layer were dominated by sequences of OTUs affiliated to the ammonia-oxidizing *Nitrososphaera* (61 ± 2%), which were also present in the original sand (53%) (Fig. 5B and Fig. SI 3).

In the inflow and outflow water samples the most abundant 16S rRNA gene sequence tags were classified into OTUs belonging to the euryarchaeal classes *Methanomicrobia* (60% inflow/48%

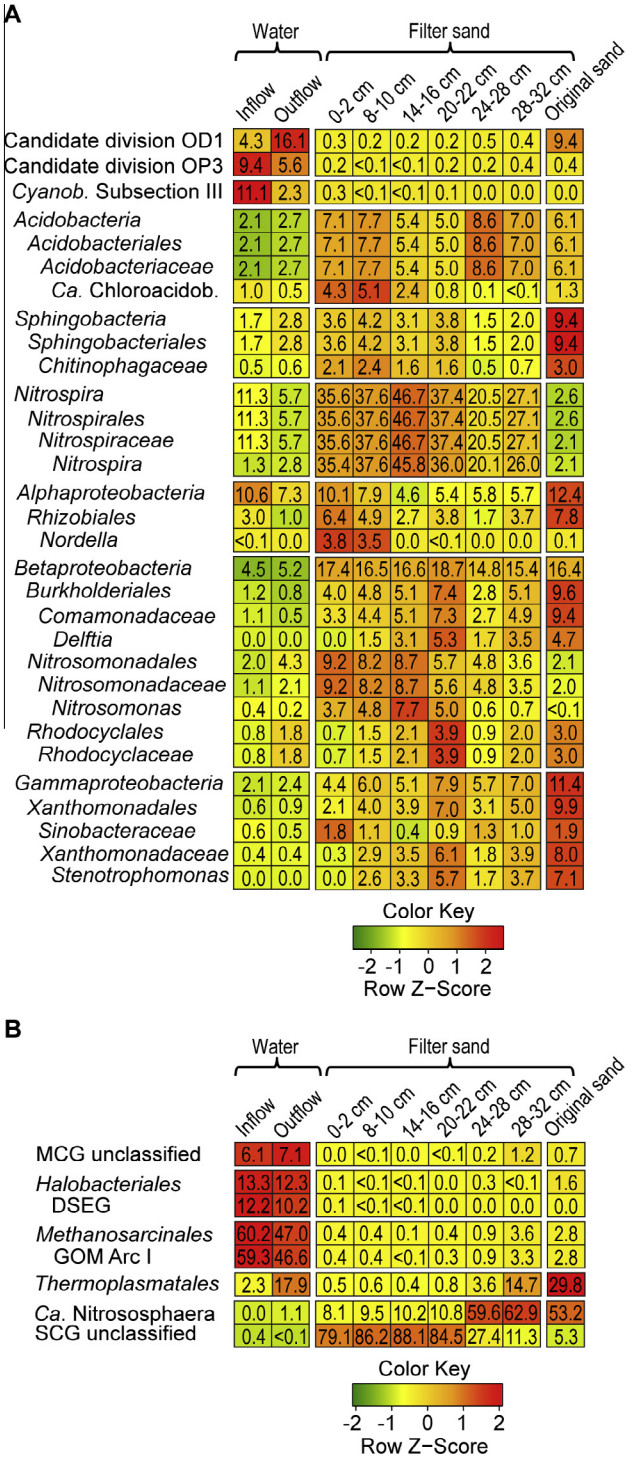

Fig. 5. Heatmaps of the most abundant taxa in the water, the filter sand, and the original sand. (A) bacterial and (B) archaeal taxa with at least >1% relative sequence abundance in one sample. Coloring according to *Z*-score. *Z*-scores represent the number of standard deviations a value differs from the mean and were used to normalize the relative taxa abundances in the different sediment layers. Positive *Z*-scores indicate values above the mean, negative *Z*-scores values below the mean. Numerical values in the heatmap represent the relative abundances of the respective taxa. A values <0.1 indicates that the relative sequence abundance was below 0.1% whereas 0.0 indicates that no sequences for the respective taxonomic group were found. Taxonomic groups are given on the phylum, order, family or genus level (*Cyanob.* Subsection III = *Cyanobacteria* Subsection III, *Ca. Chloroacidob.* = *Candidatus* Chloroacidobacterium, MCG = *Miscellaneous Crenarchaeotic Group*, DSEG = *Deep Sea Euryarcheotic Group*, SCG = *Soil Crenarchaeotic Group*, *Ca.* Nitrososphaera = "*Candidatus* Nitrososphaera").

outflow), *Halobacteria* (13%/12%), the Miscellaneous *Crenarchaeotic* Group (MCG; 6%/7%), and the *Thermoplasmata* (3%/19%) (Fig. 4B). OTUs affiliated to the *Methanosarcinales* clade GOM-Arc-1 were the dominant population in the inflow and outflow water samples (59%/47%, respectively). The Deep Sea *Euryarchaeotic* Group (DSEG) of the *Halobacteriales* accounted for 12% and 10% of the inflow and outflow water archaeal 16S rRNA gene sequences (Fig. 5B). OTUs belonging to the order *Thermoplasmatales* were detected at relatively high abundance in the original sand (30%), the white sand filter layer (15%), and the outflow water samples (18%) (Fig. 4B).

3.7. Quantification of individual taxa and functional genes

Quantitative PCRs with 16S rRNA gene group specific primers for the order *Gallionellales* and the family *Geobacteraceae* were performed to approximate the number of mIOB and IRB, respectively, in order to independently verify results obtained by MPN counts and pyrosequencing. 16S rRNA gene copy numbers g^{-1} dry sand ranged from 1×10^2 to 1×10^4 for the *Gallionellales* and 2×10^2 to 2×10^4 for the *Geobacteraceae* throughout the different layers of the sand filter. Both taxa could not be detected in the layer from 20 to 22 cm (Fig. 2B).

Pyrosequencing of 16S rRNA gene tags revealed that the filter sand is dominated by sequences of OTUs belonging to the ammonia-oxidizing bacterial taxa *Nitrosomonas* and the nitrite-oxidizing bacterial taxa *Nitrospira*. Furthermore, a relative high sequence abundance of ammonia-oxidizing archaea belonging to the thaumarchaeal taxa of unclassified SCG and *Nitrosophaera* have also been observed. In order to independently confirm the relative abundances of the different nitrifier groups in the filter sand, we performed qPCR assays using 16S rRNA gene group specific primers for *Nitrospira* sp. and functional gene specific primers for the bacterial and archaeal *amoA* genes (Fig. 2B and C). In accordance with the pyrosequencing results *Nitrospira* sp. 16S rRNA gene copy numbers were higher in the red sand layers (0–22 cm) than in the black (24–28 cm) and white (28–32 cm) sand layers (Fig. 2B and Fig. SI 4). In the red sand layers *Nitrospira* sp. 16S rRNA gene copy numbers ranged from 4 to 7×10^7 gene copies g^{-1} dry sand. Toward the bottom of the sand filter (28–32 cm) *Nitrospira* sp. 16S rRNA gene copy numbers decreased by more than an order of magnitude to 3×10^6 genes g^{-1} dry sand (Fig. 2B). In the original sand 6×10^5 *Nitrospira* sp. 16S rRNA gene copies g^{-1} dry sand were quantified (data not shown).

Bacterial *amoA* gene copy numbers fluctuated between 1×10^5 and 2×10^6 gene copies g^{-1} dry sand throughout the sand filter depth profile (Fig. 2C). Bacterial *amoA* gene copy numbers were on average an order of magnitude higher in the red sand layers than in the black and white sand layers. Thereby bacterial *amoA* gene copy numbers followed the relative sequence abundance and distribution of *Nitrosomonas* related OTUs in the filter sand (Fig. 2C and Fig. SI 4). Archaeal *amoA* gene copy numbers ranged from 3×10^6 to 8×10^7 gene copies g^{-1} dry sand in the sand filter. While archaeal *amoA* gene copy number slightly increase within the red sand layers from 2×10^7 in the top layer (0–2 cm) to 8×10^7 in the layer from 20 to 22 cm, the lowest archaeal *amoA* gene copy number were quantified in the back layer (3×10^6 - genes g^{-1} dry sand). In the white layer at the bottom of the sand filter archaeal *amoA* gene copies increased again to 2×10^7 - gene copies g^{-1} dry sand. Thereby the abundance and distribution of archaeal *amoA* gene copy numbers in the sand filter to a large extend resembles the relative abundance of thaumarchaeal 16S rRNA genes (unclassified SCG and *Nitrososphaera*) in the sand filter (Fig. 2C and Fig. SI 4). The original sand contained 3×10^5 and 4×10^6 bacterial and archaeal *amoA* gene copy numbers g^{-1} dry sand, respectively (data not shown).

The fact that we quantified higher gene copy numbers for *Nitrospira* sp. 16S rRNA and archaeal *amo*A genes compared to bacterial and archaeal 16S rRNA gene copy numbers might be due to primer specificity and the presence of multiple 16S rRNA gene operons and amoA genes in the genomes of a specific 16S rRNA gene taxa and functional gene groups, respectively.

4. Discussion

4.1. Diversity, distribution, and abundance of Fe-, Mn-, and As-oxidizing and -reducing bacteria

In this study we investigated the composition and distribution of the microbial community in a household sand filter used for the simultaneous removal of As, Fe, and Mn from contaminated groundwater. A dominant fraction of the sand filter bacterial community belonged to the *Proteobacteria* (*α*-, *β*-, *and γ*- *Proteobacteria*), *Nitrospira*, and *Acidobacteria*. These phyla have also been found to account for significant fractions of microbial communities from sand filters of full scale drinking water treatment plants (Pinto et al., 2012; White et al., 2012; Feng et al., 2013; Lin et al., 2014).

Based on theoretical calculations Voegelin et al. (2014) concluded that Fe(II) oxidation on the sand filter is dominated by autocatalytic and surface-catalyzed Fe(II) oxidation on ferrihydrite coated sand, whereas microbial Fe(II) oxidation was suggested to be of minor importance for the effective removal of As and Fe. In the context of the results presented in this study it is important to note that the detection or relative abundance of a 16S rRNA gene using DNA based analyses does not allow for conclusions to be drawn about the viability and activity of the corresponding microbial populations. However, the fact that we did not quantify any microaerophilic Fe(II)-oxidizing, and only low numbers of nitrate-reducing Fe(II)-oxidizing, Fe(III)-reducing, and Mn(IV)-reducing bacteria by MPN analysis, pyrosequencing, and qPCR is in accordance with the findings of Voegelin et al. (2014). Nonetheless, the presence of microbial taxa capable of catalyzing Fe and Mn redox reactions in the sand filter and their growth in MPN dilution cultures document that the sand filter is a habitable environment for Fe- and Mn-respiring microorganisms. Any changes to the water geochemistry, oxygen or organic carbon concentrations could promote the growth and activity of these organisms with potential consequences for Fe and Mn redox transformation and As removal efficiency of the sand filter (Kleinert et al., 2011).

Black Mn(III/IV) oxides accumulated in a distinct layer of the sand filter (24–28 cm). Voegelin et al. (2014) speculated that the slow kinetics of purely abiotic surface-catalyzed Mn oxidation might allow Mn(II)-oxidizing bacteria to take a key role in Mn removal in the sand filter. In fact, our MPN counts confirmed the presence of more than 3×10^6 Mn(II)-oxidizing bacteria g^{-1} dry sand in the black sand filter layer. Mn(II)-oxidizing bacteria are ubiquitous in nature and have been suggested to prefer environments where Mn redox cycling is rapid and without the build-up of Mn(II) or Mn(III/IV) (Tebo et al., 2005). In the sand filter, newly formed Mn(III/IV) can react quickly with reduced As and Fe and become reduced again in the process seemingly providing a preferential habitat for Mn(II)-oxidizing bacteria. Although the oxidation of Mn(II) to either Mn(III) or Mn(IV) oxides is thermodynamically favorable, Mn(II)-oxidizing bacteria have been shown to oxidize Mn enzymatically or non-enzymatically coupled to mixotrophic or heterotrophic growth with some or no energetic benefits for the organism (Ghiorse, 1984). Mn(II)-oxidizing bacteria have been identified in different phylogenetic groups in the bacterial domain and previous studies on freshwater and marine habitats classified Mn(II)-oxidizing bacterial isolates belonging to *Alpha*-, *Beta*-, *Gammaproteobacteria*, *Firmicutes*, and *Actinobacteria* (Tebo et al., 2005). For example; two Mn(II)-oxidizing bacterial cultures have been isolated from an alfisol soil (Sullivan and Koppi, 1993) and phylogenetically diverse bacterial and archaeal communities have been found in association with ferromanganese nodules in soil and sediment samples (Stein et al., 2001; Carmichael et al., 2013; Tully and Heidelberg, 2013). However, very limited information is available about microbial mechanisms and microorganisms mediating Mn oxidation in soils (He et al., 2008; Yang et al., 2013). Consistently, we did not identify any OTUs related to known Mn-oxidizing bacteria in the pyrosequencing libraries of the sand filter samples. Furthermore, none of the identified OTUs in the sand filter appeared to be exclusively enriched in the black, Mn(III/IV) oxide-rich sand layer suggesting that biotic Mn oxidation in the sand filter is most likely mediated by a phylogenetically diverse microbial community that is metabolically flexible and not solely dependent on Mn oxidation for energy generation. However, previous studies have reported that *Leptothrix* might play a major role in the removal of Mn in lab and full-scale biofilters (Li et al., 2013; Yang et al., 2014).

The microbial community composition and distribution in the sand filter are governed by the very close spatial correlation of accumulated As with ferrihydrite-like Fe(III) precipitates and separately accumulated concretions of Mn(III/IV) oxides on coated sand grains. The mineral coating of sand particles has been shown to play an important role for sand filter colonization and microbial activity (Gülay et al., 2014). Fe and As concentrations are highest in the top sand layer (0–2 cm) and decrease with filter depth (Fig. 1) (Nitzsche et al., 2015). Further down in the filter the remaining As, Fe, and also NH_4^+ and NO_2^- will be retained in a Mn(III/IV) oxide rich sand filter layer probably as a result of combined surface-catalyzed and microbial Mn(II) oxidation. Mn oxidation does not occur in the presence of NH_4^+ and NO_2^- because nitrification is energetically more favorable than Mn oxidation (Vandenabeele et al., 1995; Gouzinis et al., 1998). Therefore, the Mn oxide-rich sand layer at 24–28 cm represents a geochemical boundary layer leading to a measurable decrease of As and Fe, concentrations in the underlying sand layers and the effluent water. This geochemical transition zone has caused the development of distinct microbial communities in the red sand layers (0–22 cm) above and the white sand layer below (28–32 cm) the Mn oxide boundary layer. As mentioned above, the Mn oxide layer could be distinguished from the other sand filter layers by higher numbers of viable and culturable Mn(II)-oxidizing bacteria as quantified in MPN dilution series. Since reduced As, Fe, and nitrogen species can also abiotically reduce Mn oxides, biotic Mn oxidation and growth of Mn(II)-oxidizing bacteria will only occur once As, Fe, and NO_2^- concentrations have been sufficiently reduced (Vandenabeele et al., 1995).

Microaerophilic Fe(II)-oxidizing and Fe(III)-reducing bacteria were not present or only at relatively low cell numbers g^{-1} dry sand. MPN counts of Fe(III)-reducing bacteria and 16S rRNA gene copy numbers for the *Geobacteraceae* were in good agreement ranging between 10^3 and 10^4 cells g^{-1} dry sand. Although anaerobic growth of Fe(III)-reducing bacteria in anoxic micro niches in an overall oxic sand filter is conceivable, the low carbon content of the filter most likely restricts the growth of heterotrophs. While members of the *Gallionellales* as representative group of microaerophilic Fe(II)-oxidizing bacteria could be detected by qPCR (10^2 to 10^4 cells g^{-1} dry sand) we did not observe growth of microaerophilic Fe(II)-oxidizing bacteria in gradient tubes in a MPN dilution series. *Gallionellales* 16S rRNA sequences are consistently abundant in clone libraries from Fe mats (Gault et al., 2011; Hegler et al., 2012; Kato et al., 2012; Roden et al., 2012; Fleming et al., 2014) but they have also been found in sand filters for the treatment of

drinking water (de Vet et al., 2009; Gülay et al., 2013) or groundwater rich in As (Gorra et al., 2012; Li et al., 2013; Yang et al., 2014). However, in a recent study by (Fleming et al., 2014) on the ecological succession of Fe(II)-oxidizing bacteria in a freshwater wetland, a redundancy analysis of physicochemical parameters with Fe(II)-oxidizing bacteria abundance indicated that *Gallionellales* abundance declined in line with high concentrations of total Fe, Mn and DOC (Fleming et al., 2014). While DOC concentrations on the sand filter were low, the high Fe and Mn concentrations in the top layers of the sand filter might have constrained the growth of *Gallionella*-related microaerophilic Fe(II)-oxidizing bacteria in the sand filter.

In accordance with the MPN and qPCR results, we also found only a low relative sequence abundance of OTUs related to known Fe(II)-oxidizing bacteria in the pyrosequencing libraries of the sand filter samples (⩽0.2%, data not shown). However, modeling and co-precipitation experiments conducted by Berg et al. (2006) suggested that the efficiency of As removal in sand filters cannot fully be explained by the abiotic oxidation of Fe by atmospheric oxygen and the sorption and co-precipitation of As redox species onto and with the formed Fe(III) (oxyhydr)oxides on the sand particles. Therefore, the authors speculated that conditions present in the filter, but not considered by their modeling approach, are responsible for additional As(III) oxidation, such as redox processes involving Mn (Chiu and Hering, 2000; Tournassat et al., 2002; Voegelin et al., 2014) and the presence of As-oxidizing microorganisms (Ike et al., 2008; Kao et al., 2013). Homologs of genes encoding a respiratory arsenite oxidase (*aioA*) have been found in phylogenetically diverse microbial taxa including members of *Alpha-*, *Beta-*, *Gammaproteobacteria*, *Bacteroidetes*, *Actinobacteria*, *Firmicutes*, *Aquificae*, *Deinococcus-Thermus*, *Chlorobi*, *Chloroflexi*, *Nitrospira*, and *Crenarchaeota* (Yamamura and Amachi, 2014). *aioA*-like genes have been amplified from a variety of As-rich environments (Inskeep et al., 2007; Hamamura et al., 2009; Quemeneur et al., 2010; Sultana et al., 2012; Price et al., 2013), but they also been detected in soil or sediments containing background levels of As (Lami et al., 2013; Yamamura et al., 2013). OTUs belonging to *Proteobacteria*, *Nitrospira*, and *Crenarchaeota* comprising potential arsenite respirers were also present in the pyrosequencing libraries of the sand filter samples. Interestingly, a PCR with broad-specificity *aioA* primers provided evidence for the presence of aerobic arsenite-oxidizing bacteria in the sand filter (K.S. Nitzsche, unpublished data).

4.2. Diversity, distribution and abundance of nitrifying microorganisms

The sand filter community was to a large extent dominated by nitrifying bacteria and archaea (Figs. 4 and 5). Their occurrence is consistent with the drop in NH_4^+ from 6.4 mg L^{-1} in the groundwater to 1.6 mg L^{-1} in the filtered water and a corresponding increase in NO_3^- (up to 19 mg L^{-1} in the outflow water). Ammonium oxidation to NO_2^- and subsequent NO_2^- oxidation to NO_3^- has been demonstrated in previous studies of sand filters (Chiew et al., 2009; Murphy et al., 2010; Mangoua-Allali et al., 2012; Baig et al., 2013). While ammonia-oxidizing *Archaea* (*unclassified SCG* and *Nitrososphaera*) were more abundant than ammonia-oxidizing *Bacteria* (*Nitrosomonas*) (Fig. SI 4), the high relative abundance of a *Nitrospira defluvii*-related OTU (Fig. SI 2) suggests that NO_2^- oxidation in the sand filter is mainly associated with this taxonomic group.

Previous studies reported that *Nitrospira*, rather than *Nitrobacter*, dominate NO_2^- oxidation under conditions with low NH_4^+ and NO_2^- concentrations because *Nitrospira* have a higher affinity for NH_4^+ and a higher growth yield (Blackburne et al., 2007). The high *Nitrospira* abundance found in this study corresponds to populations described in recent studies on biological water treatment and full-scale biofilters (Martiny et al., 2005; de Vet et al., 2009; Pinto et al., 2012; Feng et al., 2013; Li et al., 2013; Lautenschlager et al., 2014; Wang et al., 2014). *Nitrospira* represents the most widespread group of known NO_2^--oxidizing bacteria found in many different aquatic and terrestrial environments, including Fe water-pipes, drinking water treatment systems, and wastewater treatment plants (Daims et al., 2001). However, knowledge on the ecophysiology of the mainly uncultured, slow-growing *Nitrospira* is limited and only two genome sequences have been obtained to date from "*Candidatus* N. defluvii" (Lücker et al., 2010) and a draft genome sequence of *N. moscoviensis* (Koch et al., 2014). Interestingly, the genome of "*Candidatus* N. defluvii" contains besides an *arsC*-type arsenate reductase, as functional component of a potential As resistant mechanism, also an *aioA*-like respiratory arsenite oxidase gene (Lücker et al., 2010). However, the growth of NO_2^--oxidizing bacteria by aerobic arsenite oxidation has not been demonstrated. Recently, growth of *N. moscoviensis* with hydrogen as electron donor has been shown, suggesting a chemolithoautotrophic lifestyle of bacterial NO_2^--oxidizers outside the nitrogen cycle (Koch et al., 2014). In the sand filter the abundance of *Nitrospira* sp. was higher in the As- and Fe-rich, red sand layers than in the filter layers below in which total As and Fe concentrations were lower (Fig. 2B and Fig. SI 4). Based on the existing genomic evidence it is intriguing to speculate that *Nitrospira* might also be capable of growing via arsenite oxidation in the sand filter thereby contributing to the As removal efficiency of the sand filter supporting the observation by Berg et al. (2006) who could not fully explain the removal efficiency by abiotic As-Fe-mineral-redox interactions. On the other hand, the abundant *Nitrospira* population in the sand filter could also be a consequence of an effective *arsC*-conferred As resistance mechanism which gives them a selective advantage over other populations at elevated As concentrations unless enough NO_2^- was available.

Our study also showed that ammonia-oxidizing archaea might play an important role in nitrification in the sand filter in addition to the well-known *Proteobacteria*. OTUs closely related to the ammonia-oxidizing *Nitrosophaera* and other soil *Thaumarchaeota* (*unclassified SCG*) were found to represent a significant part of the total archaeal population in the sand filter (Fig. 5B). The role of archaeal ammonia-oxidizers in groundwater filters for the removal of As, Fe, and, Mn is largely unknown at this time. However, previous studies have shown that members of the archaeal phylum *Thaumarchaeota* play a crucial ecological role in global nitrogen and carbon cycling (Karner et al., 2001; Francis et al., 2005; Park et al., 2006; Pester et al., 2011). Leininger et al. (2006) found that archaeal nitrifiers are more abundant than bacterial nitrifiers in different soils. The dominance of archaeal ammonia-oxidizers over bacterial ammonia-oxidizers in soils like in our sand filter might be explained by adaptation to low NH_4^+-concentrations and an autotrophic or potentially mixotrophic lifestyle (Spang et al., 2012). It is worth noting that the two dominant ammonia-oxidizing archaeal OTUs were differently distributed with sand filter depth. While the relative abundance of sequences belonging to the OTU of '*unclassified SCG*' was high in the red sand layers and decreased in the lower black Mn(III/IV) oxide rich layer and the white sand layer, the *Nitrosophaera*-related OTU showed the opposite distribution with a strong increase in relative sequence abundance in the black and white sand layers. It seems like niche occupation by different 16S rRNA gene-based lineages of *Thaumarchaeota* ammonia-oxidizing archaea might be affected by the distribution of As, Fe, and, Mn, and the availability of NH_4^+ in the sand filter. The lower As concentrations in the black and white layer could have promoted the growth of *Nitrosophaera* in these sand filter

layers. The genome of "*Candidatus* Nitrosophaera gargensis" revealed that this organism is well adapted to its niche in a heavy metal-containing thermal spring by encoding a multitude of heavy metal resistance genes but neither the presence of an As resistance mechanism nor the capability for respiratory arsenite oxidation could be confirmed by genome annotation (Spang et al., 2012).

4.3. Sand filter colonization

Overall, the sand filter microbial community was distinctly different from the groundwater microbial community. Although microorganisms from the groundwater were found in the sand filter, the microbial community of the filter still most closely resembled the microbial community of the original sand used to construct the filter, even after 8 years of continuous operation. The microbial community in the filtered water was very similar to the microbial community of the groundwater which might be due to the high flow rate (2.6 L min^{-1}) and short residence time (<30 min) of the groundwater in the sand filter (Voegelin et al., 2014) limiting the exchange and transition between planktonic and surface associated microbial populations. Recent studies on biologically active sand filters have shown that sand filter microbial biofilms are stable and resistant to perturbations and fluctuations in the source water community (Pinto et al., 2012; Lin et al., 2014). However, other engineered microbial communities have been shown to be more dynamic, quickly responding to alterations in the chemical and biological source water composition (Kaewpipat and Grady, 2002; Moons et al., 2009). Stable biofilm formation on sand particles might convey higher tolerance to As, Fe, and Mn concentrations among sand filter colonizing microbial populations compared to their freely suspended counterparts (Simões et al., 2009). In this context, continued exposure of microbial communities to high metal concentrations has been suggested to contribute to the occurrence and spread of antibiotic resistance factors in bacteria, with potential human and environmental health implications (Baker-Austin et al., 2006).

4.4. Summary

We set out to describe the composition and distribution of the microbial community in a sand filter used for the removal of As, Fe, and Mn from anoxic groundwater. We found that microorganisms capable of growing by catalyzing Fe and Mn redox transformation can be enriched from different sand layers although their relative abundance was relatively low throughout the whole filter. Mn(II)-oxidizing bacteria were found to be enriched in a distinct sand filter layer. Biotic Mn oxide formation is likely to play a key role in Mn removal but also contributes to the effective retention of As, Fe, and NH_4^+ on the sand filter. Microbial taxa comprising species potentially capable of direct arsenite oxidation were also found to be present in the sand filter. Overall, the sand filter community was clearly dominated by NO_2^--oxidizing bacteria of the phylum Nitrospira and by ammonia-oxidizing archaea of the phylum *Thaumarchaeota* suggesting an important contribution of microbial nitrification to NH_4^+ removal from the filtered groundwater. Although the mere detection and quantification of microbial taxa does not ascertain that the corresponding microorganisms are metabolically active, our analysis of the microbial community composition of the sand filter suggests that As and Fe redox transformations in the filter are to a large extent driven by abiotic processes while NH_4^+ and Mn oxidation are mainly biotic. In conclusion, it is the intricate interplay of biotic and abiotic redox transformation processes that contribute to the efficiency of the sand filter and the removal As, Fe, Mn, and NH_4^+ from the groundwater.

4.5. Implications

An understanding of the microbial processes in the sand filter that affect the geochemistry of the filtered water is critical for technology implementation and to assure consistent water quality. However, to what extent the insights on biological water treatment processes obtained from this study can be transferred to other sand filters will strongly depend on local water geochemistry, the composition of the sand used to construct the filter, and the structure and function of the seeding microbial community that comes with it.

Our findings might be relevant for the application of sand filters in centralized drinking water distribution systems (DWDS). Sand filter colonization presents a possible survival strategy for microbial communities in DWDS and these microbial communities might represent both a remediation strategy but also a potential risk for maintaining drinking water quality via sand filters. Managing sand filter microbial communities might constitute an effective alternative to control the degradation and removal of emerging bioreactive and persistent chemicals from diverse sources that are becoming more frequently detected in water resources in the pg L^{-1} and μg L^{-1} range (anthropogenic micropollutants) (Benner et al., 2013). On the other hand, biofilters as microbial habitat might constitute a potential source for undesirable microorganisms (e.g. pathogenic bacteria, corrosion or odor causing bacteria) into the downstream DWDS. Therefore it is essential to identify the forces (i.e. filter configuration, local water geochemistry) that shape the microbial community structure and its distribution within sand filters in order to derive strategies for safe and effective filter operation.

Acknowledgements

This work was founded by the German Research Foundation (DFG) to SB and AK (KA 1736/22-1). We thank Roche Diagnostics Deutschland GmbH for kindly providing the GS Junior Benchtop DNA Sequencing System. We thank Hoang Van Dung for access to the sand filter, Vi Mai Lan for her support during field work, Pham Thi Kim Trang, and Pham Hung Viet for providing lab space at CETASD, Hanoi University. We acknowledge Ellen Struve for TOC measurements, Karin Stoegerer and Marina Wüstner for help with the qPCR assays, Ankita Bhansali, Mathias Guth, and Wiebke Ruschmeier for assistance with set up and analysis of MPN counts, and Cindy Lockwood, Eva Marie Muehe, and Elizabeth Swanner for critically reading the manuscript.

Appendix A. Supplementary material

The SI includes detailed descriptions of the material and methods used for the geochemical characterization of the filter sand, the MPN counts, and the preparation of the amplicon libraries. The SI includes the following tables and figures: Table SI 1. Standards, vectors, primers and thermal profiles used in qPCR assays for different target genes; Table SI 2. pH values, water content and total organic carbon of the sand collected at different filter depths; Table SI 3. Richness estimators and diversity indices based on 97% sequence identity calculated for bacterial 16S rRNA amplicon libraries obtained from water samples, sand samples from different filter depth, and the original filter sand; Table SI 4. Richness estimators and diversity indices based on 97% sequence identity calculated for archaeal 16S rRNA amplicon libraries obtained from water samples, sand samples from different filter depth, and the original filter sand; Fig. SI 1. Rarefaction curves for 16S rRNA amplicon libraries of the different water, filter sand, and original sand samples; Fig. SI 2. Relative abundance of sequences belonging to OTUs of the phylum *Nitrospirae* from the different water, filter

sand, and original sand samples; Fig. SI 3. Relative abundance of sequences belonging to OTUs of the Soil *Crenarchaeotic* Group (SCG) in the different water, filter sand, and original sand samples; Fig. SI 4. Relative sequence abundance of the genus *Nitrosomonas* sp. the genus *Nitrospira* sp., the order "*Candidatus* Nitrososphaera" and the unclassified SCG throughout the filter. Supplementary data associated with this article can be found, in the online version, at http://dx.doi.org/10.1016/j.chemosphere.2015.05.032.

References

Baig, S.A., Sheng, T.T., Hu, Y.J., Lv, X.S., Xu, X.H., 2013. Adsorptive removal of arsenic in saturated sand filter containing amended adsorbents. Ecol. Eng. 60, 345–353.

Baker-Austin, C., Wright, M.S., Stepanauskas, R., McArthur, J.V., 2006. Co-selection of antibiotic and metal resistance. Trends Microbiol. 14 (4), 176–182.

Behrens, S., Azizian, M.F., McMurdie, P.J., Sabalowsky, A., Dolan, M.E., Semprini, L., Spormann, A.M., 2008. Monitoring abundance and expression of "*Dehalococcoides*" species chloroethene-reductive dehalogenases in a tetrachloroethene-dechlorinating flow column. Appl. Environ. Microbiol. 74 (18), 5695–5703.

Benner, J., Helbling, D.E., Kohler, H.-P.E., Wittebol, J., Kaiser, E., Prasse, C., Ternes, T.A., Albers, C.N., Aamand, J., Horemans, B., Springael, D., Walravens, E., Boon, N., 2013. Is biological treatment a viable alternative for micropollutant removal in drinking water treatment processes? Water Res. 47 (16), 5955–5976.

Berg, M., Luzi, S., Trang, P.T.K., Viet, P.H., Giger, W., Stuben, D., 2006. Arsenic removal from groundwater by household sand filters: comparative field study, model calculations, and health benefits. Environ. Sci. Technol. 40 (17), 5567–5573.

Berg, M., Trang, P.T.K., Stengel, C., Buschmann, J., Viet, P.H., Van Dan, N., Giger, W., Stüben, D., 2008. Hydrological and sedimentary controls leading to arsenic contamination of groundwater in the Hanoi area, Vietnam: the impact of iron-arsenic ratios, peat, river bank deposits, and excessive groundwater abstraction. Chem. Geol. 249 (1–2), 91–112.

Blackburne, R., Vadivelu, V.M., Yuan, Z., Keller, J., 2007. Kinetic characterisation of an enriched *Nitrospira* culture with comparison to *Nitrobacter*. Water Res. 41 (14), 3033–3042.

Bray, J.R., Curtis, J.T., 1957. An ordination of the upland forest communities of Southern Wisconsin. Ecol. Monogr. 27 (4), 325–349.

Buschmann, J., Berg, M., Stengel, C., Sampson, M.L., 2007. Arsenic and manganese contamination of drinking water resources in Cambodia: coincidence of risk areas with low relief topography. Environ. Sci. Technol. 41 (7), 2146–2152.

Carmichael, M.J., Carmichael, S.K., Santelli, C.M., Strom, A., Bräuer, S.L., 2013. Mn(II)-oxidizing bacteria are abundant and environmentally relevant members of ferromanganese deposits in caves of the upper Tennessee River Basin. Geomicrobiol. J. 30 (9), 779–800.

Chiew, H., Sampson, M.L., Huch, S., Ken, S., Bostick, B.C., 2009. Effect of groundwater iron and phosphate on the efficacy of arsenic removal by iron-amended BioSand filters. Environ. Sci. Technol. 43 (16), 6295–6300.

Chiu, V.Q., Hering, J.G., 2000. Arsenic adsorption and oxidation at manganite surfaces. 1. Method for simultaneous determination of adsorbed and dissolved arsenic species. Environ. Sci. Technol. 34 (10), 2029–2034.

Cornish, E.A., Fisher, R.A., 1938. Moments and cumulants in the specification of distributions. Revue de l'Institut International de Statistique/Rev. Int. Stat. Inst. 5 (4), 307–320.

Daims, H., Nielsen, J.L., Nielsen, P.H., Schleifer, K.-H., Wagner, M., 2001. *In Situ* characterization of *Nitrospira*-like nitrite-oxidizing bacteria active in wastewater treatment plants. Appl. Environ. Microbiol. 67 (11), 5273–5284.

de Vet, W.W.J.M., Dinkla, I.J.T., Muyzer, G., Rietveld, L.C., van Loosdrecht, M.C.M., 2009. Molecular characterization of microbial populations in groundwater sources and sand filters for drinking water production. Water Res. 43 (1), 182–194.

DeLong, E.F., 1992. Archaea in coastal marine environments. Proc. Natl. Acad. Sci. 89 (12), 5685–5689.

Dixit, S., Hering, J.G., 2003. Comparison of arsenic(V) and arsenic(III) sorption onto iron oxide minerals: implications for arsenic mobility. Environ. Sci. Technol. 37 (18), 4182–4189.

Edgar, R.C., Haas, B.J., Clemente, J.C., Quince, C., Knight, R., 2011. UCHIME improves sensitivity and speed of chimera detection. Bioinformatics 27 (16), 2194–2200.

Emerson, D., Merrill Floyd, M., 2005. Enrichment and isolation of iron-oxidizing bacteria at neutral pH. In: Jared, R.L. (Ed.), Methods in Enzymology, vol. 397. Academic Press, pp. 112–123.

Emerson, D., Moyer, C., 1997. Isolation and characterization of novel iron-oxidizing bacteria that grow at circumneutral pH. Appl. Environ. Microbiol. 63 (12), 4784–4792.

Feng, S., Chen, C., Wang, Q.F., Yang, Z.Y., Zhang, X.J., Xie, S.G., 2013. Microbial community in a full-scale drinking water biosand filter. J. Environ. Biol. 34, 321–324.

Fleming, E.J., Cetinic, I., Chan, C.S., Whitney King, D., Emerson, D., 2014. Ecological succession among iron-oxidizing bacteria. Int. Soc. Microbial Ecol. J. 8 (4), 804–815.

Francis, C.A., Roberts, K.J., Beman, J.M., Santoro, A.E., Oakley, B.B., 2005. Ubiquity and diversity of ammonia-oxidizing archaea in water columns and sediments of the ocean. Proc. Natl. Acad. Sci. U.S.A. 102 (41), 14683–14688.

Gault, A.G., Ibrahim, A., Langley, S., Renaud, R., Takahashi, Y., Boothman, C., Lloyd, J.R., Clark, I.D., Ferris, F.G., Fortin, D., 2011. Microbial and geochemical features suggest iron redox cycling within bacteriogenic iron oxide-rich sediments. Chem. Geol. 281 (1–2), 41–51.

Ghiorse, W.C., 1984. Biology of iron-and manganese-depositing bacteria. Annu. Rev. Microbiol. 38 (1), 515–550.

Gorra, R., Webster, G., Martin, M., Celi, L., Mapelli, F., Weightman, A.J., 2012. Dynamic microbial community associated with iron-arsenic co-precipitation products from a groundwater storage system in Bangladesh. Microb. Ecol. 64 (1), 171–186.

Gouzinis, A., Kosmidis, N., Vayenas, D.V., Lyberatos, G., 1998. Removal of Mn and simultaneous removal of NH_3, Fe and Mn from potable water using a trickling filter. Water Res. 32 (8), 2442–2450.

Gülay, A., Musovic, S., Albrechtsen, H.-J., Smets, B.F., 2013. Neutrophilic iron-oxidizing bacteria: occurrence and relevance in biological drinking water treatment. Water Sci. Technol.: Water Supply 13 (5), 1295–1301.

Gülay, A., Tatari, K., Musovic, S., Mateiu, R.V., Albrechtsen, H.-J., Smets, B.F., 2014. Internal porosity of mineral coating supports microbial activity in rapid sand filters for groundwater treatment. Appl. Environ. Microbiol. 80 (22), 7010–7020.

Hamamura, N., Macur, R.E., Korf, S., Ackerman, G., Taylor, W.P., Kozubal, M., Reysenbach, A.L., Inskeep, W.P., 2009. Linking microbial oxidation of arsenic with detection and phylogenetic analysis of arsenite oxidase genes in diverse geothermal environments. Environ. Microbiol. 11 (2), 421–431.

He, J., Zhang, L., Jin, S., Zhu, Y., Liu, F., 2008. Bacterial communities inside and surrounding soil iron-manganese nodules. Geomicrobiol. J. 25 (1), 14–24.

Hegler, F., Lösekann-Behrens, T., Hanselmann, K., Behrens, S., Kappler, A., 2012. Influence of seasonal and geochemical changes on iron geomicrobiology of an iron-carbonate mineral water spring. Appl. Environ. Microbiol.

Hug, S.J., Leupin, O.X., Berg, M., 2008. Bangladesh and Vietnam: different groundwater compositions require different approaches to arsenic mitigation. Environ. Sci. Technol. 42 (17), 6318–6323.

Huse, S.M., Welch, D.M., Morrison, H.G., Sogin, M.L., 2010. Ironing out the wrinkles in the rare biosphere through improved OTU clustering. Environ. Microbiol. 12 (7), 1889–1898.

Ike, M., Miyazaki, T., Yamamoto, N., Sei, K., Soda, S., 2008. Removal of arsenic from groundwater by arsenite-oxidizing bacteria. Water Sci. Technol. 58 (5), 1095–1100.

Inskeep, W.P., Macur, R.E., Hamamura, N., Warelow, T.P., Ward, S.A., Santini, J.M., 2007. Detection, diversity and expression of aerobic bacterial arsenite oxidase genes. Environ. Microbiol. 9 (4), 934–943.

Jessen, S., Larsen, F., Koch, C.B., Arvin, E., 2005. Sorption and desorption of arsenic to ferrihydrite in a sand filter. Environ. Sci. Technol. 39 (20), 8045–8051.

Kaewpipat, K., Grady Jr., C.P.L., 2002. Microbial population dynamics in laboratory-scale activated sludge reactors. Water Sci. Technol. 46 (1–2), 19.

Kao, A.-C., Chu, Y.-J., Hsu, F.-L., Liao, V.H.-C., 2013. Removal of arsenic from groundwater by using a native isolated arsenite-oxidizing bacterium. J. Contam. Hydrol. 155, 1–8.

Karner, M.B., DeLong, E.F., Karl, D.M., 2001. Archaeal dominance in the mesopelagic zone of the Pacific Ocean. Nature 409 (6819), 507–510.

Kato, S., Kikuchi, S., Kashiwabara, T., Takahashi, Y., Suzuki, K., Itoh, T., Ohkuma, M., Yamagishi, A., 2012. Prokaryotic abundance and community composition in a freshwater iron-rich microbial mat at circumneutral pH. Geomicrobiol J. 29 (10), 896–905.

Klee, A.J., 1993. A computer program for the determination of most probable number and its confidence limits. J. Microbiol. Methods 18 (2), 91–98.

Kleinert, S., Muehe, E.M., Posth, N.R., Dippon, U., Daus, B., Kappler, A., 2011. Biogenic Fe(III) minerals lower the efficiency of iron-mineral-based commercial filter systems for arsenic removal. Environ. Sci. Technol., 7533–7541

Koch, H., Galushko, A., Albertsen, M., Schintlmeister, A., Gruber-Dorninger, C., Lücker, S., Pelletier, E., Le Paslier, D., Spieck, E., Richter, A., Nielsen, P.H., Wagner, M., Daims, H., 2014. Growth of nitrite-oxidizing bacteria by aerobic hydrogen oxidation. Science 345 (6200), 1052–1054.

Lami, R., Jones, L.C., Cottrell, M.T., Lafferty, B.J., Ginder-Vogel, M., Sparks, D.L., Kirchman, D.L., 2013. Arsenite modifies structure of soil microbial communities and arsenite oxidization potential. FEMS Microbiol. Ecol. 84 (2), 270–279.

Lane, D.J., 1991. 16S/23S rRNA sequencing. In: Stackebrandt, E., Godfellow, M. (Eds.), Nucleic Acid Techniques in Bacterial Systematics. John Wiley & Son Ltd., New York, pp. 115–175.

Lautenschlager, K., Hwang, C., Ling, F., Liu, W.-T., Boon, N., Köster, O., Egli, T., Hammes, F., 2014. Abundance and composition of indigenous bacterial communities in a multi-step biofiltration-based drinking water treatment plant. Water Res. 62, 40–52.

Learman, D.R., Wankel, S.D., Webb, S.M., Martinez, N., Madden, A.S., Hansel, C.M., 2011. Coupled biotic–abiotic Mn(II) oxidation pathway mediates the formation and structural evolution of biogenic Mn oxides. Geochim. Cosmochim. Acta 75 (20), 6048–6063.

Leininger, S., Urich, T., Schloter, M., Schwark, L., Qi, J., Nicol, G.W., Prosser, J.I., Schuster, S.C., Schleper, C., 2006. Archaea predominate among ammonia-oxidizing prokaryotes in soils. Nature 442 (7104), 806–809.

Li, X.-K., Chu, Z.-R., Liu, Y.-J., Zhu, M.-T., Yang, L., Zhang, J., 2013. Molecular characterization of microbial populations in full-scale biofilters treating iron, manganese and ammonia containing groundwater in Harbin, China. Bioresour. Technol. 147, 234–239.

Lin, W., Yu, Z., Zhang, H., Thompson, I.P., 2014. Diversity and dynamics of microbial communities at each step of treatment plant for potable water generation. Water Res. 52, 218–230.

Liu, Z., Lozupone, C., Hamady, M., Bushman, F.D., Knight, R., 2007. Short pyrosequencing reads suffice for accurate microbial community analysis. Nucleic Acids Res. 35 (18), e120.
Luan, F., Santelli, C.M., Hansel, C.M., Burgos, W.D., 2012. Defining manganese(II) removal processes in passive coal mine drainage treatment systems through laboratory incubation experiments. Appl. Geochem. 27 (8), 1567–1578.
Lücker, S., Wagner, M., Maixner, F., Pelletier, E., Koch, H., Vacherie, B., Rattei, T., Damsté, J.S.S., Spieck, E., Le Paslier, D., Daims, H., 2010. A *Nitrospira* metagenome illuminates the physiology and evolution of globally important nitrite-oxidizing bacteria. Proc. Natl. Acad. Sci. 107 (30), 13479–13484.
Mandal, B.K., Suzuki, K.T., 2002. Arsenic round the world: a review. Talanta 58 (1), 201–235.
Mangoua-Allali, A.L.C., Coulibaly, L., Ouattara, J.-M.P., Gourene, G., 2012. Implementation of biosand filters in rural area for drinking water production. Afr. J. Food Sci. 6 (24).
Martiny, A.C., Albrechtsen, H.J., Arvin, E., Molin, S., 2005. Identification of bacteria in biofilm and bulk water samples from a nonchlorinated model drinking water distribution system: detection of a large nitrite-oxidizing population associated with *Nitrospira* spp. Appl. Environ. Microbiol. 71 (12), 8611–8617.
Melton, E.D., Rudolph, A., Behrens, S., Schmidt, C., Kappler, A., 2014a. Influence of nutrient concentrations on MPN quantification and enrichment of nitrate-reducing Fe(II)-oxidizing and Fe(III)-reducing bacteria from littoral freshwater lake sediments. Geomicrobiol. J. 31 (9), 788–801.
Melton, E.D., Swanner, E.D., Behrens, S., Schmidt, C., Kappler, A., 2014b. The interplay of microbially mediated and abiotic reactions in the biogeochemical Fe cycle. Nat. Rev. Micro 12 (12), 797–808.
Moons, P., Michiels, C.W., Aertsen, A., 2009. Bacterial interactions in biofilms. Crit. Rev. Microbiol. 35 (3), 157–168.
Muehe, E.M., Kappler, A., 2014. Arsenic mobility and toxicity in the environment – a review on biogeochemistry, health and socio-economic effects, remediation and future predictions. Environ. Chem.
Murphy, H.M., McBean, E.A., Farahbakhsh, K., 2010. A critical evaluation of two point-of-use water treatment technologies: can they provide water that meets WHO drinking water guidelines? J. Water Health 8 (4).
Muyzer, G., de Waal, E.C., Uitterlinden, A.G., 1993. Profiling of complex microbial populations by denaturing gradient gel electrophoresis analysis of polymerase chain reaction-amplified genes coding for 16S rRNA. Appl. Environ. Microbiol. 59 (3), 695–700.
Nitzsche, K.S., Lan, V.M., Trang, P.T.K., Viet, P.H., Berg, M., Voegelin, A., Planer-Friedrich, B., Zahoransky, J., Müller, S.-K., Byrne, J.M., Schröder, C., Behrens, S., Kappler, A., 2015. Arsenic removal from drinking water by a household sand filter in Vietnam – effect of filter usage practices on arsenic removal efficiency and microbiological water quality. Sci. Total Environ. 502, 526–536.
Oremland, R.S., Stolz, J.F., 2003. The ecology of arsenic. Science 300 (5621), 939–944.
Pace, N.R., Stahl, D.A., Lane, D.J., Olsen, G.J., 1986. The analysis of natural microbial populations by reibosomal RNA sequences. In: Marshall, K.C. (Ed.), Advances in Microbial Ecology. Springer, US, pp. 1–55.
Park, H.-D., Wells, G.F., Bae, H., Criddle, C.S., Francis, C.A., 2006. Occurrence of ammonia-oxidizing archaea in wastewater treatment plant bioreactors. Appl. Environ. Microbiol. 72 (8), 5643–5647.
Pester, M., Schleper, C., Wagner, M., 2011. The Thaumarchaeota: an emerging view of their phylogeny and ecophysiology. Curr. Opin. Microbiol. 14 (3), 300–306.
Pinto, A.J., Xi, C., Raskin, L., 2012. Bacterial community structure in the drinking water microbiome is governed by filtration processes. Environ. Sci. Technol. 46 (16), 8851–8859.
Postma, D., 1985. Concentration of Mn and separation from Fe in sediments—I. Kinetics and stoichiometry of the reaction between birnessite and dissolved Fe(II) at 10 °C. Geochim. Cosmochim. Acta 49 (4), 1023–1033.
Price, R.E., Lesniewski, R., Nitzsche, K.S., Meyerdierks, A., Saltikov, C., Pichler, T., Amend, J., 2013. Archaeal and bacterial diversity in an arsenic-rich shallow-sea hydrothermal system undergoing phase separation. Front. Microbiol. 4.
Pruesse, E., Quast, C., Knittel, K., Fuchs, B.M., Ludwig, W., Peplies, J., Glöckner, F.O., 2007. SILVA: a comprehensive online resource for quality checked and aligned ribosomal RNA sequence data compatible with ARB. Nucleic Acids Res. 35 (21), 7188–7196.
Quemeneur, M., Cebron, A., Billard, P., Battaglia-Brunet, F., Garrido, F., Leyval, C., Joulian, C., 2010. Population structure and abundance of arsenite-oxidizing bacteria along an arsenic pollution gradient in waters of the upper Isle River Basin, France. Appl. Environ. Microbiol. 76 (13), 4566–4570.
Quince, C., Lanzen, A., Curtis, T.P., Davenport, R.J., Hall, N., Head, I.M., Read, L.F., Sloan, W.T., 2009. Accurate determination of microbial diversity from 454 pyrosequencing data. Nat. Methods 6 (9), 639–641.
Roden, E., McBeth, J.M., Blothe, M., Percak-Dennett, E.M., Fleming, E.J., Holyoke, R.R., Luther, G.W., Emerson, D., 2012. The microbial ferrous wheel in a neutral pH groundwater seep. Front. Microbiol. 3.
Salama, I.A., Koch, G.G., Tolley, H.D., 1978. On the estimation of the most probable number in a serial dilution technique. Commun. Stat. – Theory Methods A7, 1267–1281.
Schloss, P.D., Handelsman, J., 2005. Introducing DOTUR, a computer program for defining operational taxonomic units and estimating species richness. Appl. Environ. Microbiol. 71 (3), 1501–1506.
Schloss, P.D., Westcott, S.L., 2011. Assessing and improving methods used in operational taxonomic unit-based approaches for 16S rRNA gene sequence analysis. Appl. Environ. Microbiol. 77 (10), 3219–3226.
Schloss, P.D., Westcott, S.L., Ryabin, T., Hall, J.R., Hartmann, M., Hollister, E.B., Lesniewski, R.A., Oakley, B.B., Parks, D.H., Robinson, C.J., Sahl, J.W., Stres, B., Thallinger, G.G., Van Horn, D.J., Weber, C.F., 2009. Introducing mothur: open-source, platform-independent, community-supported software for describing and comparing microbial communities. Appl. Environ. Microbiol. 75 (23), 7537–7541.
Schloss, P.D., Gevers, D., Westcott, S.L., 2011. Reducing the effects of PCR amplification and sequencing artifacts on 16S rRNA-based studies. PLoS ONE 6 (12), e27310.
Simões, M., Simões, L.C., Vieira, M.J., 2009. Species association increases biofilm resistance to chemical and mechanical treatments. Water Res. 43 (1), 229–237.
Spang, A., Poehlein, A., Offre, P., Zumbrägel, S., Haider, S., Rychlik, N., Nowka, B., Schmeisser, C., Lebedeva, E.V., Rattei, T., Böhm, C., Schmid, M., Galushko, A., Hatzenpichler, R., Weinmaier, T., Daniel, R., Schleper, C., Spieck, E., Streit, W., Wagner, M., 2012. The genome of the ammonia-oxidizing *Candidatus* Nitrososphaera gargensis: insights into metabolic versatility and environmental adaptations. Environ. Microbiol. 14 (12), 3122–3145.
Stein, L.Y., La Duc, M.T., Grundl, T.J., Nealson, K.H., 2001. Bacterial and archaeal populations associated with freshwater ferromanganous micronodules and sediments. Environ. Microbiol. 3 (1), 10–18.
Straub, K.L., Kappler, A., Schink, B., 2005. Enrichment and isolation of ferric-iron- and humic-acid-reducing bacteria. In: Jared, R.L. (Ed.), Methods in Enzymology, vol. 397. Academic Press, pp. 58–77.
Sullivan, L., Koppi, A., 1993. Manganese oxide accumulations associated with some soil structural pores. II. Composite coatings and translocation. Soil Res. 31 (3), 227–233.
Sultana, M., Vogler, S., Zargar, K., Schmidt, A.-C., Saltikov, C., Seifert, J., Schlömann, M., 2012. New clusters of arsenite oxidase and unusual bacterial groups in enrichments from arsenic-contaminated soil. Arch. Microbiol. 194 (7), 623–635.
Tebo, B.M., Bargar, J.R., Clement, B.G., Dick, G.J., Murray, K.J., Parker, D., Verity, R., Webb, S.M., 2004. Biogenic manganese oxides: properties and mechanisms of formation. Annu. Rev. Earth Planet. Sci. 32 (1), 287–328.
Tebo, B.M., Johnson, H.A., McCarthy, J.K., Templeton, A.S., 2005. Geomicrobiology of manganese(II) oxidation. Trends Microbiol. 13 (9), 421–428.
Tebo, B.M., Clement, B.G., Dick, G.J., 2007. Biotransformations of manganese. In: Hurst, C.J., Crawford, R.L., Garland, J.L., Lipson, D.A., Mills, A.L., Stetzenbach, L.D. (Eds.), Manual of environmental microbiology, third ed. ASM Press, Washington, DC, pp. 1223–1238.
Tournassat, C., Charlet, L., Bosbach, D., Manceau, A., 2002. Arsenic(III) oxidation by birnessite and precipitation of manganese(II) arsenate. Environ. Sci. Technol. 36 (3), 493–500.
Tully, B.J., Heidelberg, J.F., 2013. Microbial communities associated with ferromanganese nodules and the surrounding sediments. Front. Microbiol. 4.
van Beek, C.G.E.M., Hiemstra, T., Hofs, B., Nederlof, M.M., Van Paassen, J.A.M., Reijnen, G.K., 2012. Homogeneous, heterogeneous and biological oxidation of iron(II) in rapid sand filtration. J. Water Supply: Res. Technol.-AQUA 61 (1), 1–13.
Vandenabeele, J., Vande Woestyne, M., Houwen, F., Germonpré, R., Vandesande, D., Verstraete, W., 1995. Role of autotrophic nitrifiers in biological manganese removal from groundwater containing manganese and ammonium. Microb. Ecol. 29 (1), 83–98.
Villinski, J.E., O'Day, P.A., Corley, T.L., Conklin, M.H., 2001. *In situ* spectroscopic and solution analyses of the reductive dissolution of MnO_2 by Fe(II). Environ. Sci. Technol. 35 (6), 1157–1163.
Voegelin, A., Kaegi, R., Berg, M., Nitzsche, K.S., Kappler, A., Lan, V.M., Trang, P.T.K., Göttlicher, J., Steininger, R., 2014. Solid-phase characterisation of an effective household sand filter for As, Fe and Mn removal from groundwater in Vietnam. Environ. Chem. 11 (5), 566–578.
Wang, Q., Garrity, G.M., Tiedje, J.M., Cole, J.R., 2007. Naïve Bayesian Classifier for rapid assignment of rRNA sequences into the new bacterial taxonomy. Appl. Environ. Microbiol. 73 (16), 5261–5267.
Wang, H., Narihiro, T., Straub, A.P., Pugh, C.R., Tamaki, H., Moor, J.F., Bradley, I.M., Kamagata, Y., Liu, W.-T., Nguyen, T.H., 2014. MS2 Bacteriophage reduction and microbial communities in biosand filters. Environ. Sci. Technol. 48 (12), 6702–6709.
White, C.P., DeBry, R.W., Lytle, D.A., 2012. Microbial survey of a full-scale, biologically active filter for treatment of drinking water. Appl. Environ. Microbiol. 78 (17), 6390–6394.
Winkel, L.H.E., Pham, T.K.T., Vi, M.L., Stengel, C., Amini, M., Nguyen, T.H., Pham, H.V., Berg, M., 2011. Arsenic pollution of groundwater in Vietnam exacerbated by deep aquifer exploitation for more than a century. Proc. Natl. Acad. Sci. U.S.A. 108 (4), 1246–1251.
Yamamura, S., Amachi, S., 2014. Microbiology of inorganic arsenic: from metabolism to bioremediation. J. Biosci. Bioeng. 118 (1), 1–9.
Yamamura, S., Watanabe, K., Suda, W., Tsuboi, S., Watanabe, M., 2013. Effect of antibiotics on redox transformations of arsenic and diversity of arsenite-oxidizing bacteria in sediment microbial communities. Environ. Sci. Technol. 48 (1), 350–357.

Yang, W., Zhang, Z., Zhang, Z., Chen, H., Liu, J., Ali, M., Liu, F., Li, L., 2013. Population structure of manganese-oxidizing bacteria in stratified soils and properties of manganese oxide aggregates under manganese–complex medium enrichment. PLoS ONE 8 (9), e73778.
Yang, L., Li, X., Chu, Z., Ren, Y., Zhang, J., 2014. Distribution and genetic diversity of the microorganisms in the biofilter for the simultaneous removal of arsenic, iron and manganese from simulated groundwater. Bioresour. Technol. 156, 384–388.
Ying, S.C., Kocar, B.D., Fendorf, S., 2012. Oxidation and competitive retention of arsenic between iron- and manganese oxides. Geochim. Cosmochim. Acta 96, 294–303.
Zhao, S., Fernald, R.D., 2005. Comprehensive algorithm for quantitative real-time polymerase chain reaction. J. Comput. Biol. 12 (8), 1047–1064.
Zhou, J.Z., Bruns, M.A., Tiedje, J.M., 1996. DNA recovery from soils of diverse composition. Appl. Environ. Microbiol. 62 (2), 316–322.